

The APM Survey for Cool Carbon Stars in the Galactic Halo - II The Search for Dwarf Carbon Stars.

E. J. Totten,¹ M. J. Irwin² and P.A. Whitelock³

¹*Department of Physics, Keele University, Keele, Staffordshire, ST5 5BG, UK*

²*Institute of Astronomy, Madingley Road, Cambridge CB3 1HA, UK*

³*South African Astronomical Observatory, P.O. Box 9, 7935 Observatory, S. Africa*

Draft version

ABSTRACT

We present proper motion measurements for carbon stars found during the APM Survey for Cool Carbon Stars in the Galactic Halo (Totten & Irwin, 1998). Measurements are obtained using a combination of POSSI, POSSII and UKST survey plates supplemented where necessary by CCD frames taken at the Isaac Newton Telescope. We find no significant proper motion for any of the new APM colour-selected carbon stars and so conclude that there are no dwarf carbon stars present within this sample. We also present proper motion measurements for three previously known dwarf carbon stars and demonstrate that these measurements agree favourably with those previously quoted in the literature, verifying our method of determining proper motions. Results from a complimentary program of JHK photometry obtained at the South African Astronomical Observatory are also presented. Dwarf carbon stars are believed to have anomalous near-infrared colours, and this feature is used for further investigation of the nature of the APM carbon stars. Our results support the use of JHK photometry as a dwarf/giant discriminator and also reinforce the conclusion that none of the new APM-selected carbon stars are dwarfs. Finally, proper motion measurements combined with extant JHK photometry are presented for a sample of previously known Halo carbon stars, suggesting that one of these stars, CLS29, is likely to be a previously unrecognised dwarf carbon star.

Key words: stars: carbon – stars: surveys – astrometry: stars – infrared: stars

1 INTRODUCTION

Until recently it was believed that all faint high-latitude carbon (FHLC) stars were giants. Since main sequence stars do not produce carbon, it was assumed that faint carbon stars were distant examples of the classical, bright carbon giants. Recently, however a new and growing class of so-called dwarf carbon stars has been discovered (see Green 1996 for a recent review). Dwarf carbon stars are believed to be binary systems, where the dwarf carbon star has received material from a now “invisible” companion during the ascent of the companion star up the asymptotic giant branch (Dahn *et al.* 1977). Preliminary parallax studies indicate that dwarf carbon stars have the luminosity of late main sequence dwarfs (Dearborn *et al.* 1986, Harris *et al.* 1998) but also mimic the overall spectral characteristics of carbon giants. Dwarf carbon stars are recognisable by their relatively high proper motions and it has been suggested (Green *et al.* 1991) that they have anomalous JHK near-infrared colours. Spectroscopically, the distinction between dwarf and giant

carbon stars is less obvious – it has been suggested by Green *et al.* (1992) that the spectra of dwarf carbon stars contain an enhanced C_2 bandhead at 6191 Å which is correspondingly less pronounced in the spectra of giant carbon stars.

The APM Survey for cool carbon stars in the Galactic Halo (Totten & Irwin 1998) found 48 carbon stars with $11 \lesssim R \lesssim 17$; $B_J - R \gtrsim 2.4$, and at Galactic latitudes $|b| > 30^\circ$. While there is not enough gas and dust present at such high latitudes to support recent star formation, the question of the origin of such carbon stars is an on-going question. We have suggested that these carbon stars provide observational evidence of recent tidal disruption of dwarf satellite galaxies in the Galactic Halo (Totten & Irwin 1998, Irwin & Totten 1999). We argue that many of the Halo carbon stars are the tidal debris of such merging events, and as such may prove to be excellent probes of the outer Halo. However, it should also be born in mind that the current sample may be contaminated by less distant, dwarf carbon stars, which would play no part in such a scenario. It is

Table 1. Measured proper motions for a selection of dwarf carbon stars and previously published faint high latitude carbon stars.

Name	Coord (B1950)	1 st Epoch (POSSI)	2 nd Epoch (POSSII/UKST)	Baseline (yr)	μ_α (arcsec/yr)	μ_δ (arcsec/yr)	Notes
Dwarf							
G77-61	0330+0148	E932	R11438	32.9	+0.199 ± 0.006	-0.740 ± 0.007	1
		E932	SJ01677	34.1	+0.191 ± 0.006	-0.750 ± 0.006	
PG0824	0824+2853	E1351	SJ03130	35.0	-0.022 ± 0.006	-0.001 ± 0.005	2
CLS50	1217+3704	E1599	SJ01744	31.9	-0.077 ± 0.007	-0.019 ± 0.007	3
FHLC							
C*01	0002+0053	E319	R7939	30.9	-0.010 ± 0.009	+0.001 ± 0.007	4
C*03	0108-0015	E1259	OR11269	31.8	-0.004 ± 0.008	+0.002 ± 0.008	4
		E1259	SJ03587	35.9	-0.006 ± 0.008	-0.002 ± 0.009	
Green et al.	0311+0733	E1471	SJ03564	34.8	+0.000 ± 0.004	-0.003 ± 0.006	5
CLS26	1025+2923	E1387	SJ01033	31.8	+0.009 ± 0.008	+0.004 ± 0.008	6
CLS43	1135+3321	E109	SJ01730	37.8	-0.003 ± 0.008	+0.000 ± 0.007	6
CLS45	1149+3727	E109	SJ01730	37.8	+0.002 ± 0.007	+0.000 ± 0.007	6
CLS54	1231+3625	E105	SJ01744	37.8	+0.001 ± 0.009	-0.007 ± 0.008	6
CLS57	1239+3122	E64	SJ03131	39.9	-0.009 ± 0.008	-0.003 ± 0.008	6
CLS80	1415+2936	E70	SJ04486	42.0	+0.002 ± 0.008	-0.014 ± 0.007	6
CLS98	1605+2922	E134	SJ03297	40.0	-0.008 ± 0.007	+0.008 ± 0.006	6
CLS112	1706+3316	E1132	SJ01967	34.0	+0.014 ± 0.006	-0.011 ± 0.006	6
C*02	2354+0021	E319	R7939	31.0	+0.001 ± 0.009	-0.001 ± 0.007	7

Notes : 1 Dahn *et al.* 1977; 2 Heber *et al.* 1993; 3 Green *et al.* 1992; 4 Bothun *et al.* 1991; 5 Green *et al.* 1994; 6 Sanduleak & Pesch 1988; 7 Bothun *et al.* 1991.

therefore essential that every precaution is taken to exclude dwarf carbon stars from the putative distant Halo carbon star sample and with that in mind we have carried out a series of proper motion measurements on: the APM carbon star sample; a selection of known dwarf carbon stars to verify the method; and a sample of other FHLC stars.

In Section 2 we describe how proper motions were measured for each carbon star and show how such measurements can readily be used to statistically separate dwarf from giant carbon stars. Section 3 describes the near-infrared photometry program carried out on the 1.9m at the South African Astronomical Observatory (SAAO) and how this has been applied to the classification of dwarf and giant carbon stars. Section 3 also includes a description of how the JHK photometric data can be used to estimate distances for the APM carbon stars.

2 PROPER MOTIONS

The typical transverse velocity of Halo stars, including the effects of reflex solar motion and the intrinsic velocity dispersion in the Halo, is $\approx 150 \text{ kms}^{-1}$. At a distance of 20 kpc – a canonical distance for a Halo carbon star of magnitude $R \approx 13.0$ and with $M_R = -3.5$, this would translate to an expected proper motion of $\sim 1.5 \text{ mas/yr}$. On the other hand, a Halo dwarf carbon star of this apparent magnitude and with $M_R \approx +9$ (Harris *et al.* 1998) would be at a distance of around 100 pc and would be expected to have a proper motion of $\approx 300 \text{ mas/yr}$. Even with disk kinematics the ex-

pected proper motion of a dwarf carbon star would be $\approx 100 \text{ mas/yr}$. Clearly then, measuring proper motions should be a very powerful way of distinguishing between dwarf and giant carbon stars.

Suitable first epoch plate material is provided by the red glass copies (Ennnn in Tables 1,2) of the first Palomar Sky Survey (POSSI) undertaken during the 1950s. For the second epoch, a mixture of the available second Palomar Sky Survey (POSSII) IIIaJ glass copies or IIIaF film copies (SJnnnn, SFnnnn in Tables 1,2), and UK Schmidt Telescope (UKST) original plates (Rnnnn or ORnnnn in Tables 1,2), obtained during the late 1980s and early 1990s, provided most of the material. In addition, for some of the northern hemisphere APM carbon stars we obtained second epoch data on the 2.5m Isaac Newton Telescope (INT) on La Palma. The INT data were taken in April 1997 using the first incarnation of the INT Wide Field Camera, with $2k \times 2k$ thinned Loral CCDs. The target fields were centred on the best of the two working devices giving a field coverage of $12.5 \times 12.5 \text{ arcmin}$, at a spatial sampling of $0.37 \text{ arcsec/pixel}$. An R-band filter was used to provide a match to the first epoch red plates and exposure times between 50s and 100s were used to avoid saturating the target image.

Much of the required plate material had already been measured on the APM facility (Kibblewhite *et al.* 1984) as part of the APM sky survey catalogues (Irwin & McMahon 1992, Irwin *et al.* 1994). Any remaining second epoch POSSII plates were also measured and processed in the same way. The baseline difference between the two epochs for the plate material is generally between 30–40 years, rising to well over 40 years for the CCD data (see Tables 1, 2). The CCD data was preprocessed (bias-corrected, trimmed and flat-fielded)

Table 2. Measured Proper Motions for APM colour-selected faint high latitude carbon stars.

Name	1 st Epoch	2 nd Epoch	Baseline	μ_α (arcsec/yr)	μ_δ (arcsec/yr)
0000+3021	E1257	SJ05402	38.9	-0.002 ± 0.007	-0.002 ± 0.004
0102-0556	E1206	OR13284	35.0	+0.006 ± 0.008	-0.003 ± 0.009
0123+1233	E635	SJ01389	34.7	-0.003 ± 0.006	+0.004 ± 0.007
0207-0211	E825	R8222	29.1	+0.009 ± 0.009	+0.003 ± 0.007
0217+0056	E1283	R8284	29.0	-0.003 ± 0.009	-0.008 ± 0.008
0222-1337 ³	E886	R7240	27.9	+0.015 ± 0.012	+0.013 ± 0.007
0225+2634	E858	SJ04231	37.9	+0.008 ± 0.008	-0.001 ± 0.006
0316+1006	E11	SF04359	42.0	+0.001 ± 0.005	-0.004 ± 0.006
0340+0701	E1499	SF03652	34.9	-0.006 ± 0.006	-0.005 ± 0.005
0351+1127	E940	SF02252	34.9	+0.000 ± 0.006	-0.002 ± 0.007
0357+0908	E1308	SF02252	34.0	+0.001 ± 0.004	-0.001 ± 0.005
0418+0122	E1524	OR14085	35.4	+0.001 ± 0.005	+0.004 ± 0.005
0713+5016	E670	SF02976	36.8	-0.003 ± 0.004	-0.002 ± 0.005
0748+5404 ³	E985	SF06135	41.0	-0.025 ± 0.004	-0.015 ± 0.005
0748+7221 ³	E680 ¹	CCD	44.1		
0911+3341	E1342	CCD	42.1	+0.012 ± 0.006	+0.009 ± 0.007
0915-0327	E430	R8400	31.2	+0.010 ± 0.008	+0.006 ± 0.006
0936-1008	E1536	OR11832	31.4	+0.001 ± 0.006	+0.001 ± 0.005
0939+3630	E925	CCD	43.3	-0.005 ± 0.007	+0.005 ± 0.003
1013+7340	E685	CCD	44.1	+0.004 ± 0.004	+0.001 ± 0.002
1019-1136	E1537	OR9900	29.1	+0.015 ± 0.009	+0.007 ± 0.007
1037+3603	E731	SF02321	35.8	+0.035 ± 0.006	-0.050 ± 0.006
1037+2616	E1380	CCD	42.0	+0.003 ± 0.005	+0.002 ± 0.003
1056+4000	E1349	SJ03815	35.9	+0.005 ± 0.009	+0.003 ± 0.008
1123+3723	E695	SJ03164	37.1	-0.004 ± 0.007	-0.007 ± 0.007
1130-1020	E1562	OR12389	31.9	+0.001 ± 0.007	+0.010 ± 0.006
1211-0844	E1023	OR10243	31.2	+0.013 ± 0.008	+0.005 ± 0.006
1225-0011	E1405	OR12996	33.8	+0.008 ± 0.011	+0.000 ± 0.007
1241+0237	E104	R5032	29.1	-0.009 ± 0.009	+0.001 ± 0.009
	E104	SJ03232	40.0	-0.010 ± 0.010	-0.003 ± 0.008
1249+0146	E1578	R5032	23.3	+0.011 ± 0.009	+0.003 ± 0.009
	E1578	SJ03232	34.2	+0.002 ± 0.007	+0.000 ± 0.010
1254-1130	E1591	OR13095	33.1	+0.013 ± 0.010	-0.001 ± 0.009
1339-0700	E500	OR9964	32.8	+0.019 ± 0.008	+0.005 ± 0.008
1350+0101	E465	R6808	29.1	+0.007 ± 0.010	+0.003 ± 0.009
1406+0520	E96	CCD	47.0	+0.012 ± 0.009	-0.002 ± 0.007
1429-0518	E1062	R9158	29.9	+0.013 ± 0.007	-0.001 ± 0.008
1442-0058	E1613	R5774	22.9	-0.001 ± 0.011	-0.003 ± 0.010
1450-1300	E1025	OR11939	32.8	+0.006 ± 0.007	+0.001 ± 0.006
1509-0902	E1431	OR14962	37.0	+0.003 ± 0.008	-0.003 ± 0.006
1511-0342	E1431	R6979	26.0	+0.003 ± 0.010	+0.004 ± 0.008
1519-0614	E1431	R6979	26.0	+0.003 ± 0.010	-0.004 ± 0.009
1523+4235	E1376	SF05116	38.0	-0.012 ± 0.006	+0.005 ± 0.007
2111+0010	E575	OR13307	37.1	+0.006 ± 0.005	+0.002 ± 0.005
	E575	SJ03390	37.9	+0.001 ± 0.007	+0.001 ± 0.008
2213-0017	E1146	OR11414	32.2	+0.005 ± 0.008	+0.001 ± 0.008
	E1146	SJ02069	34.0	+0.002 ± 0.011	-0.001 ± 0.006
2223+2548	E817	SJ02069	34.1	+0.003 ± 0.009	-0.005 ± 0.008
2225-1401	E1180	OR13265	35.0	+0.011 ± 0.010	+0.000 ± 0.008
2229+1902	E842	SJ03396	36.8	+0.011 ± 0.007	+0.002 ± 0.007
2255+0556	E821	SJ03416	36.9	+0.000 ± 0.008	-0.002 ± 0.009
2259+1249 ³	E800 ²	SF04266	38.1		

Notes :

1. Image is elliptical and unresolved on plate E680.
2. Image is elliptical and unresolved on plate E800.
3. These four Carbon stars brighter than the APM survey limit: 0222-1337; 0748+5404; 0748+7221; 2259+1249 have been included here for completeness.

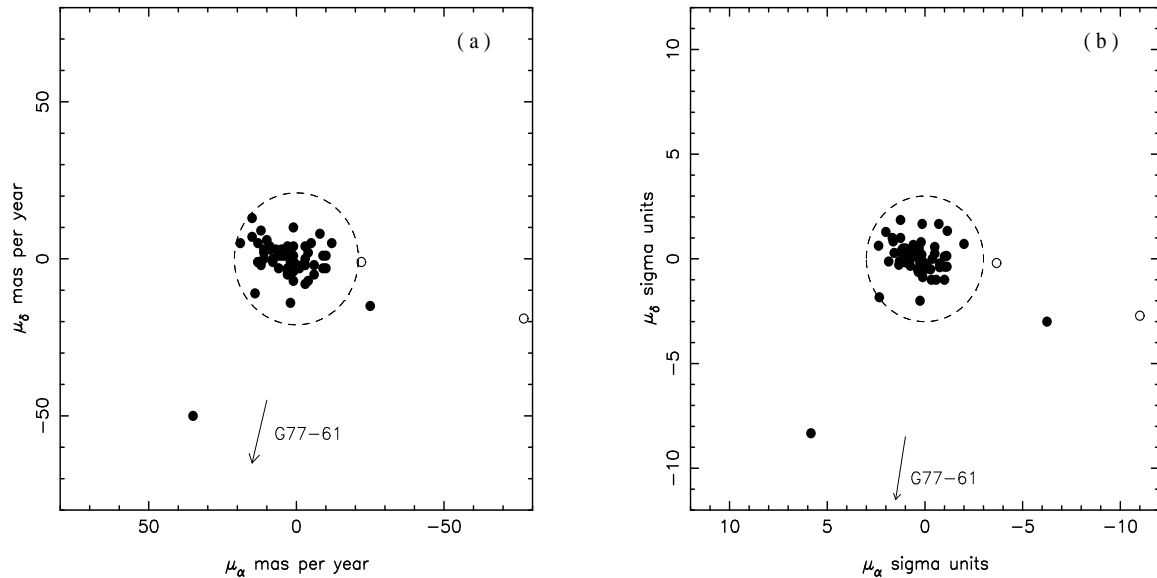


Figure 1. (a) measured carbon star proper motions in mas/yr. The dashed line shows the average 3σ limit for proper motion measurements (21 mas/yr). The three dwarf carbon stars lie outside this boundary, with G77-61 lying outside the limits of the plot. (b) the distribution of carbon star proper motions normalised by the error estimate for each measurement. The dashed line again shows the 3σ limit for proper motions. Stars outside this boundary have significant proper motions and were subject to further investigation to determine if they are dwarf carbon stars. Dwarf carbon stars are plotted as open circles, all other carbon stars are shown as filled circles.

in the standard manner and then an object detection and parameterisation algorithm, similar to that run on the APM, was used to generate an object list.

Second epoch plates were also scanned around any previously published FLHC stars, not in the APM survey (eg. Totten & Irwin 1998 Table 1) and of several known dwarf carbon stars, wherever suitable plate material was readily available. Derived proper motions for this extra subset were then used to check for any previously overlooked dwarf carbon stars in the non-APM FHLC sample, and the published proper motions of the known dwarf carbon stars (eg. Deutsch 1994) were used to provide a benchmark to assess the external accuracy of our derived proper motions.

2.1 Procedure

The output from the measuring process, including the CCD data, is a list of detected objects together with a parameterisation including: x-y coordinates, flux, and morphological information. All plate/CCD matching was performed in the natural plate-based coordinate system of the data. Derived proper motion estimates were then transformed to a celestial system using the usual APM plate-based astrometric calibration. All images on both reference (generally second epoch) and comparison material were iteratively matched using a general linear 6 plate constant coordinate transform over a region of 20×20 arcmin, centred on the target carbon star, for the photographic data and 12.5×12.5 arcmin for the CCD data. The linear transform allows for shifts, rotation and scaling differences between the two epochs. Any slight bias in the internally derived proper motion zero-point

from using all images on the plates is negligible < 1 mas/yr compared to the anticipated proper motion of dwarf carbon stars and also much smaller than the random individual measuring error for each carbon star.

The linear transformation between 1st and 2nd epoch was derived using a least-squares fit between matched coordinates of the two datasets. $3\text{-}\sigma$ clipping (where $\sigma = 1.48 \times$ median absolute difference of the coordinates) was used to reject outliers. The least-square fits were then repeated iteratively using $3\text{-}\sigma$ clipping until all matched transformed objects lie within $3\text{-}\sigma$ of their associated positions on the reference system.

The proper motion of the target carbon star (μ_α and μ_δ in arcsec/yr) is then simply the difference between the carbon star positions on the 1st and 2nd epoch plates (or CCD frames), normalised by the epoch difference. The typical accuracy of the positional difference estimate between two plates is ~ 0.27 arcsec for stellar images and is dominated by the random errors of the individual star measurements. The accuracy of the internally-derived zero-point, which was typically based on ≈ 100 objects, is better than 1 mas/yr, again much smaller than any expected dwarf carbon star proper motion. For a baseline of $\sim 30 - 40$ years the corresponding error on the derived carbon star proper motion is approximately 5-10 mas/yr on each coordinate.

2.2 Proper Motion Results

Tables 1, 2 list the derived proper motions for the sample studied here. Proper motion estimates have already been determined for the three dwarf carbon stars included in Table 1, by Dahn *et al.* (1977), Green *et al.* (1991) and Heber *et*

al. (1993). Included in Table 1 are our estimates for several previously published “normal” FHLC stars (eg. Sanduleak & Pesch 1988, Bothun *et al.* 1991 and Green *et al.* 1992). Table 2 lists estimates for the majority of the APM Survey carbon stars listed in Totten & Irwin (1998). The two bright objects, $R < 11$, without a proper motion estimate in Table 2 are blended with neighbouring images on the 1st epoch POSSI plate, making it impossible to accurately measure the position of the carbon star. The other two bright images are included in the table for completeness.

The distribution of proper motions is plotted in Figure 1. Panel 1a shows the distribution of the proper motions of the stars as measured, where the dashed line corresponds to the average $3\text{-}\sigma$ error for the proper motion measurements (~ 21 mas/yr). Any star with a significant proper motion will lie outside this line. Panel 1b shows the distribution of carbon stars proper motions normalised by the individual σ for each measurement. The dashed line again represents the notional $3\text{-}\sigma$ boundary between a null detection of proper motion and stars having a significant proper motion. The three dwarf carbon stars are denoted by open circles or arrows and are outside the $3\text{-}\sigma$ boundary on both panels. All other carbon stars are shown as filled circles. Most lie well within the null proper motion boundary and only two fall outside of it, highlighting the simplicity of this approach for statistically identifying dwarf proper motion candidates and also for ruling out the dwarf hypothesis for the majority of the sample.

2.3 The Dwarf Carbon Stars

PG0824+2853 lies just outside the $3\text{-}\sigma$ boundary in Figure 1., but even so would have been a good candidate for a dwarf carbon star based on this position. Previous determinations of the proper motion reported by Heber *et al.* (1993) and by Deutsch (1994) of $-0.028, 0.002$ and $-0.036, 0.000$ respectively, agree within the errors with our value of $-0.022, -0.001$ arcsec/yr. As suggested by previous authors, this relatively low proper motion is more consistent with a disk population dwarf carbon star, rather than a Halo star.

CLS50 has a significant proper motion which places it near the edge of the plot in Figure 1a,b. Green *et al.* (1992) first reported this object as a dwarf carbon star and estimated its proper motion to be $-0.068, -0.013$ arcsec/yr. Deutsch (1994) re-estimated the proper motion and found a result in excellent agreement with the above of $-0.069, -0.012$ and in good agreement with our derived value of $-0.077, -0.019$ arcsec/yr.

G77-61 is off the scale on both panels of the figure. However, our value for the proper motion of $0.195, -0.745$ agrees well with previous determinations by Dearborn *et al.* (1986) and by Deutsch (1994) of $0.189, -0.749$ and $0.184, -0.745$ respectively. Both G77-61 and CLS50 have the high proper motions expected from Halo population objects

We conclude from this brief comparison that our error estimates of between $5\text{--}10$ mas/yr for the derived proper motions, based on internal statistical considerations, provide realistic absolute proper motion errors.

2.4 Other Outliers – A New Dwarf Carbon Star

With the exception of two stars, all of the FHLC stars studied lie well within the $3\text{-}\sigma$ boundary and have relatively insignificant proper motion, leading us to conclude that none of them are dwarf carbon stars.

Of the two stars lying outside the $3\text{-}\sigma$ boundary: 0748+5404 is a bright CH-type carbon star previously reported in Stephenson’s catalogue of cool carbon stars (Stephenson 1989) and re-observed during the APM Survey. The brightness of this object means that the diffraction spikes are clearly visible on both the POSSI and POSSII plates and that it is heavily saturated on both plates. This leads to larger than average centroiding errors and hence the apparently significant proper motion is misleading. On further visual examination of the plate material by digitally blinking pixel maps of the pair of images, we cannot detect any obvious motion at the 1 arcsec level and therefore conclude that this star is probably not a dwarf carbon star.

CLS29=1037+3603 on the other hand is a much fainter carbon star, previously discovered by Sanduleak & Pesch (1988) and re-observed during the APM survey. We have detected a significant proper motion for this star of $\mu_\alpha = +0.035 \pm 0.006$ and $\mu_\delta = -0.050 \pm 0.006$. Over a 35.8 yr baseline this corresponds to a total motion of 2.2 arcsec and should be readily visible to the eye. To check this an 8×8 arcmin region centred on the carbon star was digitised at $1/2$ arcsec sampling for the red POSSI glass plate copy and the red POSSII film copy using the APM facility. The resulting pixel maps were coaligned in a similar manner to that described previously, using the POSSI image as reference, and using a bilinear interpolation to transform the POSSII image onto the reference system. Figure 2 shows a 5×5 arcmin sub-region centred on the carbon star for each plate. CLS29 has clearly moved relative to the majority of faint images, which are expected to have negligible proper motion. Other relatively bright images also show proper motion between the frames but this is to be expected given the baseline between the plates.

Green *et al.* (1992) previously investigated a sample of the then known FHLC stars and found CLS29 to not have a significant proper motion. However, their $3\text{-}\sigma$ proper motion limit of $\approx 60\text{--}70$ mas/yr is a factor of three greater than our limit of ≈ 20 mas/yr. With a total proper motion of 61 mas/yr (at PA 145°), CLS29, was marginally below their detection limit. Such a low value for the proper motion is characteristic of disk population dwarf carbon stars and we suspect that CLS29 may be an additional member of that class.

We can place additional constraints on the nature of CLS29 by combining the measured value for the proper motion with our published values for the radial velocity and B_J, R magnitudes (Totten & Irwin 1998). At Galactic coordinates of $l = 187.4$, $b = 60.8$, CLS29 lies within 30 degrees of the North Galactic pole and hence the low heliocentric radial velocity of $V_h = -3 \pm 6$ km/s is indicative of a low value for the Z component of the Galactocentric velocity, consistent with disk membership.

The colour transformations described in Irwin *et al.* (1990) and the measured photographic magnitudes for CLS29 of $R = 14.3$ and $B_J = 16.4$, imply $V = 15.2$. With the

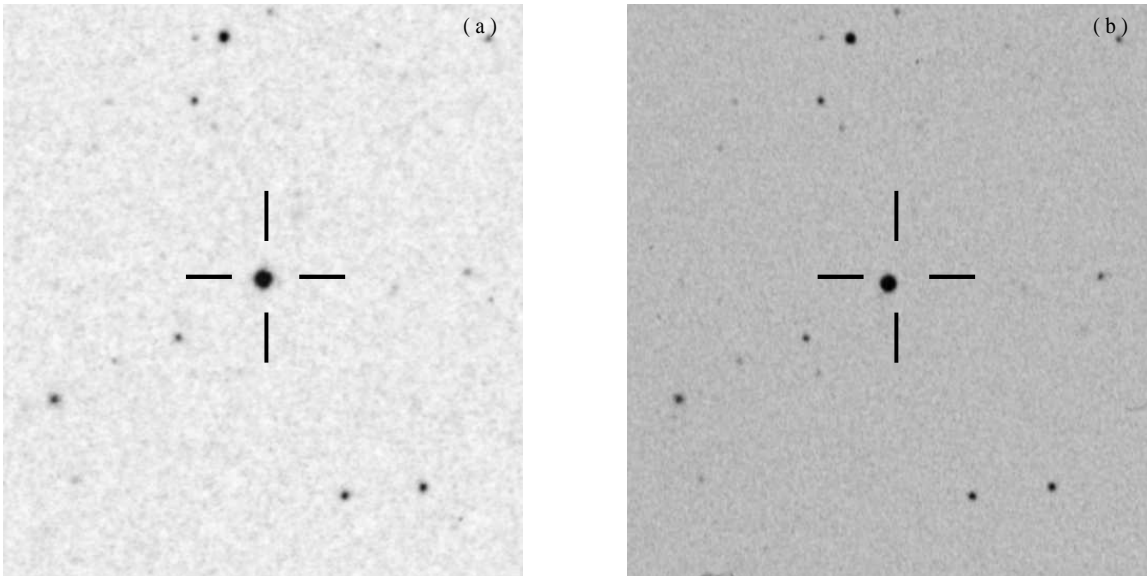


Figure 2. 5×5 arcmin images of the dwarf carbon star CLS29. (a) is taken from a scan of the POSSI (first epoch) plate while (b) is taken from a scan of the POSSII (second epoch) film copy. The images have the conventional orientation with North to the top and East to the left of the images. The first epoch position is marked by a cross in each of the images and it is clear that the position of CLS29, relative to faint background objects, has changed over the 35.8 year baseline between these two observations.

caveat of low number statistics, the dwarf carbon stars with measured parallaxes have a luminosity distribution in the range $9.6 < M_V < 10.0$ (Harris et al. 1998), suggesting a distance for CLS29 of approximately 120 pc. Combining the proper motion, radial velocity and estimated distance yields the following Galactocentric components of velocity, $(U, V, W) \approx (34, 210, 16)$, indicative of disk membership. The spectrum of CLS29, Figure 5. of Totten & Irwin (1998), is also unusual. Detailed examination of the spectrum reveals no obvious counterpart to the enhanced C_2 bandhead at 6191\AA , that Green et al. (1992) have suggested is indicative of dwarf carbon stars. Conventionally, CLS29 is a CH-type carbon star. However, it also has an unambiguous $H\alpha$ emission line superimposed on the usual carbon star spectral features. Although not uncommon in N-type carbon stars from our sample, CLS29 is the only CH-type carbon star we observed that has Balmer lines in emission. For N-type carbon stars, Balmer emission has been attributed to strong chromospheric activity or Mira-like shock waves, in CH-type stars however, it is more likely to indicate mass transfer or a similar interaction between the dwarf carbon star and its now invisible binary companion (eg. a faint white dwarf). Future UV observations might confirm the presence of the white dwarf and hence the binary nature of CLS29. Finally, as we show in the next section, CLS29 has JHK colours that lie close to the zone containing the known dwarf carbon stars with extant JHK photometry. Taking all the evidence together strongly suggests that CLS29 is a dwarf carbon star and that it is highly likely to be a member of the disk population of dwarf carbon stars.

3 NEAR-INFRARED JHK PHOTOMETRY

Green *et al.* (1992) and Westerlund *et al.* (1995) have suggested that dwarf carbon stars have anomalous infrared

colours. Higher gravities and lower metallicities encourage the association of hydrogen, thereby reducing the opacity in the H-band and driving the locus of dwarf carbon star colours away from the normal carbon star locus in conventional two-colour JHK diagrams.

With this in mind a program to obtain near-infrared JHK (1.25μ , 1.65μ , 2.2μ) photometry for all the previously published carbon stars, visible from SAAO, was started during 1996, using the Mk III infrared photometer on the 1.9m telescope at SAAO. Observations were transformed to the SAAO photometric system using standards taken from Carter (1990). The mean JHK magnitudes for the carbon stars observed at SAAO are listed in Table 3. Associated errors for each magnitude measurement are in the range ± 0.01 – 0.02 mag for the majority of the observations, rising to 0.05 – 0.1 mag for those denoted by “:”. Several of the stars were observed on more than one occasion and were found to be variables. In these cases the average magnitude is quoted in Table 3. The repeat observations, variability and periods of such stars will be the subject of a forth-coming paper. The pertinent issue here is the luminosity class, which can be considered using the average magnitudes.

Combining the new observations with previously published JHK photometry transformed to the SAAO system (see Carter 1990), for both the dwarf carbon stars and FHLC stars (see Table 1. of Totten & Irwin 1998) yields the two-colour diagram in $J-H$ -v- $H-K$ shown in Figure 3, where we have neglected the effects of extinction. All of the optically classified N-type stars in these tables are plotted as open circles, all CH-type stars as filled circles and all previously known dwarf carbon stars are plotted as dots inside open circles. As expected there is an excellent discrimination in colour between the locii of CH-type and N-type carbon stars, confirming the original optical classification. Although the dwarf carbon star population generally lies below the locus of normal carbon stars, there is some overlap with the dis-

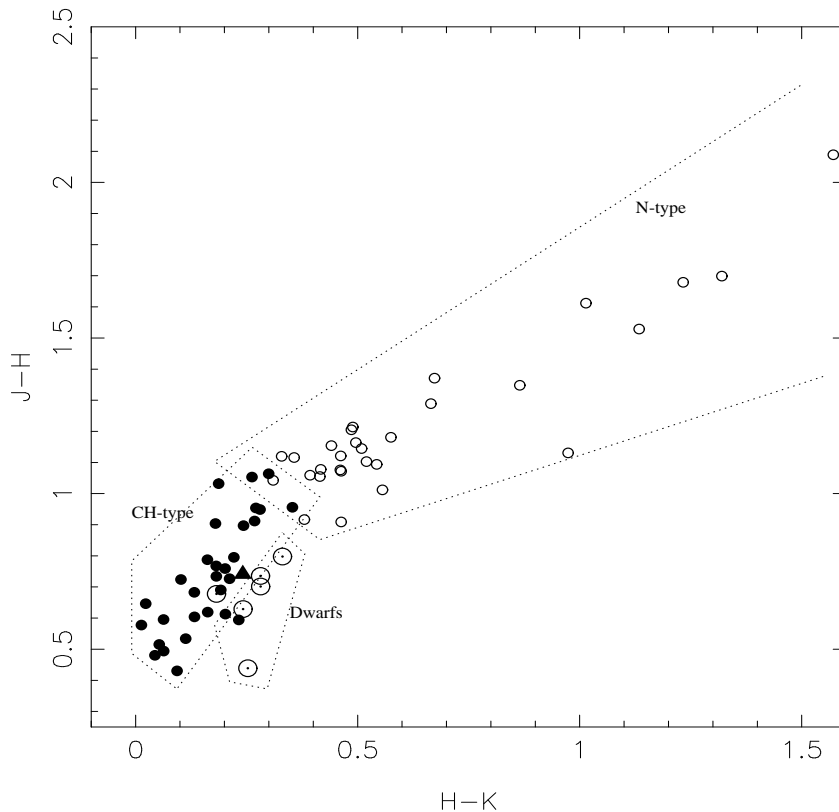


Figure 3. A two colour JHK diagram for all the FHLC stars with extant near-infrared photometry. Optically classified N-type carbon stars are plotted as open circles, CH-type carbon stars are plotted as filled circles and dwarf carbon stars are plotted as dots inside open circles. The superimposed dotted boundaries illustrate the loci of the separate carbon star types. The newly discovered dwarf carbon star, CLS29=1037+3603, is plotted as a filled triangle and lies close to the region occupied by the known dwarf carbon stars.

tribution of normal carbon giants. From the diagram it is apparent that:

- the bluer and more common CH-type stars, mainly from the earlier FHLC sample, almost exclusively populate the bottom left hand corner of the figure.
- N-type carbon stars, which are also much redder optically (eg. Totten & Irwin 1998), are generally well separated from the CH-type stars and occupy the upper right hand section of the diagram. Mira variables will fall along a general loci similar to that of the N-type carbon stars, however most Miras are extremely red and so we would expect them to lie in the extreme top-right section of the plot, with some falling outside the boundary of the diagram. Both from repeat variability measurements and from their position in the carbon star locus, several of the N-type carbon stars are likely to be carbon-rich Miras.
- dwarf carbon stars, for which significant proper motions have been measured, are seen to occupy a smaller section of the diagram, along the red edge of the CH-type population. They are unambiguously separated from the N-type population.
- CLS29, the newly identified dwarf carbon star, plotted as a filled triangle in the figure, lies on the boundary between the CH-type and dwarf domains. PG0824+2853, which has

a visible DA white dwarf companion possibly affecting the JHK photometry, lies inside the CH-type zone.

So although the JHK colour alone is insufficient evidence to guarantee membership of the dwarf carbon star class, it does act as a useful secondary indicator when combined with the proper motion measurements. JHK colour, however, does give a good indication of generic carbon star type with a well-defined boundary between CH and N-type stars.

Several of the stars in the list presented in Table 3. of Totten & Irwin (1998) had uncertain classification based solely on optical data. Of these: 0351+1127 with J-H,H-K colours of 1.12,0.33 lies just inside the N-type zone; 0936-1008 at 1.21,0.49 is well inside the N-type zone; and 1339-0700 at 0.96,0.35 lies on the boundary between CH and N-type;

Westerlund *et al.*(1995) defined dwarf carbon stars as having $J-H < 0.75$, $H-K > 0.25$ mag, using the transformations of Bessell & Brett 1988, these become 0.76 and 0.26 respectively in the SAAO system, similar to that seen in Figure 3. This gives a clear separation between N-type and dwarf carbon star populations, and shows independently of the proper motion measurements, that none of the N-type carbon stars found during the APM Survey are likely to be dwarf carbon stars. CLS29=1037+3603, which has colours

Table 3. Infrared photometry of FLHC stars obtained at SAAO

Name	J	H	K		Comments
0002+0053	11.11	10.35	10.10	C*01	CH-type
0100–1619	13.14:	12.59:	12.51:	C*23	CH-type
0102–0556	11.34	9.74	8.60	C*07 + APM	N-type +em lines, variable – Mira ?
0108–0015	13.55:	12.84:	12.77:	C*03	CH-type
0123+1233	9.85	8.89	8.62	Stephenson + APM	CH-type
0207–0211	11.25	10.33	9.90	C*30 + APM	N-type variable – Mira ?
0217+0056	11.34	10.23	9.82	C*31 + APM	N-type
0222–1337	7.45	6.38	6.09	C*15	CH-type IRAS FSC
0225+2634	10.50	9.28	8.79	APM	N-type
0228–0256	12.57	11.81	11.63	C*08	CH-type
0229–0316	11.95	11.02	10.69	C*09	CH-type
0311+0733	14.01:	13.032	12.87:	Green et al. 1994	CH-type
0316+1006	10.51	9.62	9.37	APM	CH-type
0340+0701	9.97	8.81	8.37	APM	N-type
0351+1127	11.82	10.70	10.37	APM	N-type
0357+0908	12.79	11.61	11.26	APM	N-type
0418+0122	10.07	7.98	6.41	APM	N-type +dust – Mira ? IRAS PSC2.0
0915–0327	9.97	8.91	8.65	APM	CH-type
0936–1080	12.41	11.20	10.72	APM	N-type
1019–1136	10.09	9.00	8.45	APM	N-type
1025+2923	12.29	11.70	11.64:	CLS26	CH-type
1037+2616	11.34	10.28	9.88	APM	N-type
1130–1020	7.39	5.23	3.63	IRAS + APM	N-type +dust – Mira ?
1211–0844	13.19	12.28	11.82	APM	N-type +em lines – Mira ?
1220+2122	11.59	10.45	9.94	Moody et al. +APM	N-type
1225–0011	12.27	11.13	10.16	APM	N-type – Mira ?
1241+0237	12.93	11.86	11.39	UM515 + APM	N-type
1249+0146	12.76	11.42	10.55	APM	N-type – Mira ?
1252+1017	12.16	11.48	11.31	CLS67	CH-type
1254–1130	10.94	9.89	9.47	APM	N-type
1339–0700	10.52	9.56	9.21	APM	CH/N-type
1350+0101	12.73	11.55	10.97	APM	N-type
1406+0520	8.84	7.74	7.22	Stephenson + APM	N-type
1415+2936	10.82	10.33	10.17	CLS80	CH-type
1429–0518	13.94:	12.26	11.03	APM	N-type +dust – Mira ?
1442–0058	12.22	11.14	10.68	APM	N-type
1450–1300	13.90:	12.29	11.27	APM	N-type – Mira ?
1511–0342	12.83:	11.82	11.26	APM	N-type
1519–0614	13.26	12.09	11.60	APM	N-type
1525+2912	13.60:	12.80	12.76:	CLS87	CH-type
1605+2922	10.78	10.13	10.01	CLS98	CH-type
2111+0010	12.60	11.70	11.52	APM	CH-type
2213–0017	10.91	9.83	9.41	APM	N-type
2213–1451	12.13	11.22	11.03	C*26	CH-type
2223+2548	7.65	5.95	4.63	Stephenson + APM	N-type +dust, em lines – Mira ? IRAS PSC2.0
2225–1401	12.13	10.76	10.09	APM	N-type variable – Mira ?
2229+1902	10.89	9.77	9.31	APM	N-type
2255+0556	10.63	9.71	9.45	APM	CH-type
2259+1249	7.11	5.83	5.16	Stephenson + APM	N-type +em lines
2305–1356	14.38:	13.75:	13.80:	C*13	CH-type
2346+0248	13.14:	12.40:	12.26:	C*10	CH-type
2354+0021	13.46	13.09:	12.81:	C*02	CH-type

Note : See Tables 1 and 3, Totten & Irwin 1998 for further details.

on the SAAO system of $J-H = 0.74$, $H-K = 0.27$ lies close to the putative dwarf carbon star zone defined by Westerlund *et al.*.

3.1 Calibrating distances

Over the same period as the photometric observations of the FLHC stars were taken, a similar set of photometry was recorded (one dataset by MJI, the other by PAW & MWF) for a series of cool N-type carbon stars in the outer

Table 5. Photometric distances in kpc for all carbon stars with extant infrared photometry.

Name	M_K	d_{\odot} (JHK)	Name	M_k	d_{\odot} (JHK)
0002+0053	-6.1	18	1231+3625	-5.9	9
0100-1619	-3.9	20	1239+3122	-5.2	7
0102-0556	-8.8	30	1241+0237	-7.7	66
0108-0015	-5.0	35	1249+0146	-8.5	65
0123+1233	-6.9	13	1252+1017	-5.4	22
0207-0211	-7.3	27	1254-1130	-7.6	26
0217+0056	-7.7	31	1313+3535	-5.5	25
0222-1337	-7.3	5	1339-0700	-7.2	19
0225+2634	-8.0	23	1350+0101	-8.1	64
0228-0256	-5.8	31	1406+0520	-7.9	10
0229-0316	-7.0	35	1415+2936	-4.1	7
0311+0733	-6.6	80	1429-0518	-8.8	94
0316+1006	-6.6	16	1442-0058	-7.7	47
0340+0701	-7.8	17	1450-1300	-8.7	101
0351+1127	-7.5	38	1509-0902	-5.8	117
0357+0908	-7.7	62	1511-0342	-7.8	64
0418+0122	-8.9	12	1519-0614	-7.9	80
0911+3341	-4.2	9	1523+4235	-8.6	20
0915-0327	-7.2	15	1525+2912	-5.3	41
0936-1080	-8.0	55	1532+3242	-5.9	25
0939+3630	-3.6	21	1605+2922	-4.9	9
1015+3540	-5.2	26	1637+3437	-4.1	16
1019-1136	-7.9	19	1706+3316	-3.1	15
1025+2923	-4.1	14	2111+0010	-6.4	39
1037+2616	-7.5	30	2213-0017	-7.6	25
1037+3603			2223+2548	-8.9	5
1123+3723	-6.0	11	2225-1401	-8.4	50
1130-1020	-9.0	3	2229+1902	-7.8	26
1135+3321	-5.0	32	2255+0556	-6.8	18
1149+3727	-5.2	13	2259+1249	-8.3	5
1211-0844	-7.3	68	2305-1356	-7.8	35
1213+3721	-3.1	9	2346+0248	-5.5	36
1220+2122	-7.9	37	2354+0021	-4.1	24
1225-0011	-8.4	53			

parts of the SMC and LMC. This combined dataset proved extremely valuable in attempting to calibrate carbon star distances derived from JHK photometry.

The process of calibrating stellar distances from near-infrared photometry of carbon stars relies heavily on the fact that the distances to several nearby Galactic satellite systems are well defined and also that these dwarf satellite galaxies contain populations of carbon stars of similar nature to those found in the Halo surveys. A compilation of carbon stars with published JHK photometry was made for the Galactic dwarf spheroidal satellites: Fornax, Carina, Sculptor, Ursa Minor, Draco, Leo I and Leo II, and was combined with the aforementioned LMC and SMC carbon star sample, supplemented by some additional LMC and SMC carbon star studies with JHK photometry. The photometric data for the dwarf spheroidals was taken from the literature. Relevant information and references are given in Table 4. All measurements were again transformed to the SAAO photometric system as necessary (Glass 1985) using the equations

of Carter (1990) and Bessell and Brett (1988). The distance moduli used were taken from a review by Van den Bergh (1989) and are also given in Table 4. Extinction corrections in the K-band are less than 0.02 mag for all the carbon stars considered and we have therefore ignored the effects of extinction throughout. Figure 4 shows the derived absolute K-band magnitude for each carbon star as a function of its J-K colour. Distance moduli for all stars were assumed to be the same as for the parent galaxy – the values quoted in Table 4 are used in the interest of using a consistent distance scale, since in this context small systematic recalibration of the absolute distance is not of crucial importance. In all of the following analysis we have also neglected the effects of intervening extinction, for both the calibrating carbon stars and the Halo sample, since for both samples the estimated JHK Galactic extinction is negligible compared to other sources of uncertainty.

The Hartwick and Cowley (1988) sample of bright CH-type carbon stars have been included in Figure 4, using the

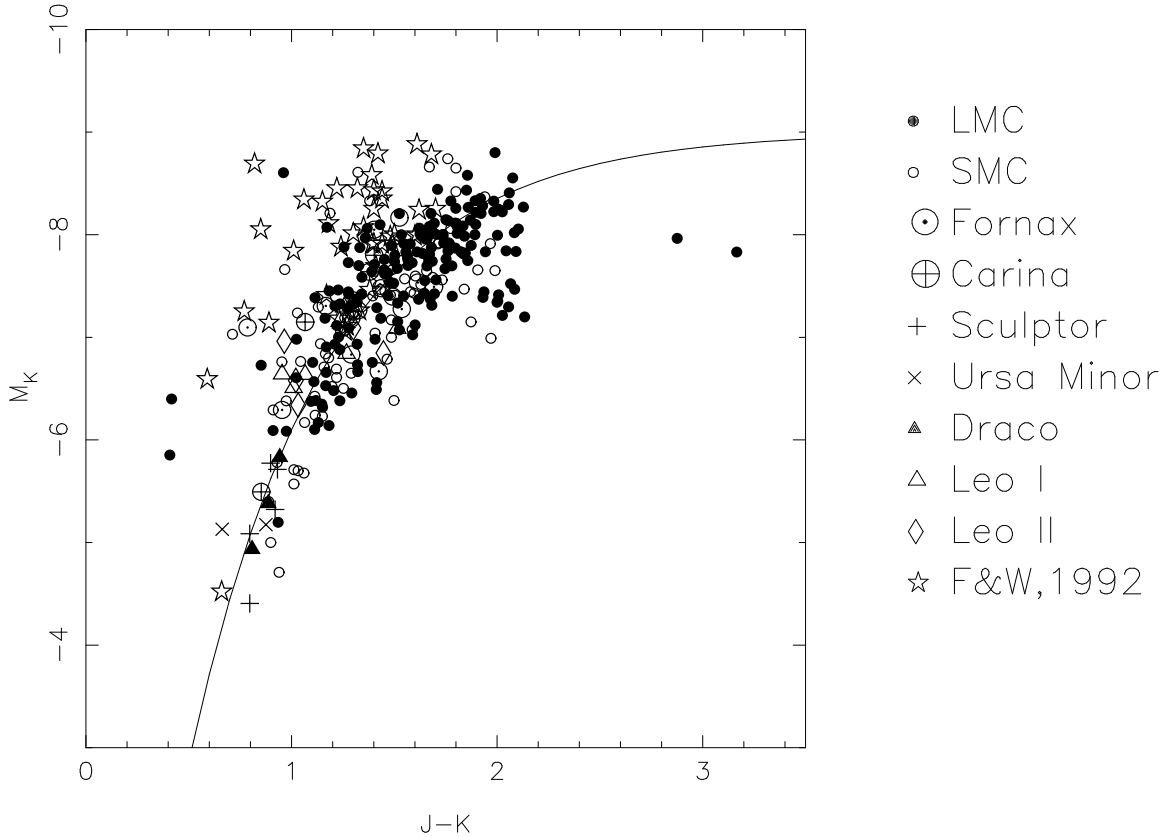


Figure 4. Colour Magnitude diagram showing the relationship between $J-K$ and M_K for the compilation of carbon stars referred to in Table 4, including local group galaxies for which J,H,K photometry was found in the literature. The overplotted curve is an empirical fit to the data used to JHK distances to the FHLC star sample. The F&W 1992 values refer to JHK measurements of the Hartwick and Cowley (1988) sample of bright LMC CH-type carbon stars.

JHK photometry from Feast & Whitelock (1992). (Much of the Suntzeff *et al.* JHK photometry for the Hartwick & Cowley sample is extrapolated from measurements in R and I, therefore we have used only the Feast & Whitelock measurements in the figure.) As already noted by several authors, these carbon stars appear to be significantly brighter and/or bluer than the majority of LMC carbon stars in NIR colour-magnitude diagrams. Suntzeff *et al.* 1993 argued that the extant spectroscopic, photometric and kinematic data, provided a compelling case for these objects being associated with a much younger (10^8 years) population of AGB stars compared to the "normal" LMC carbon population (although see Costa & Frogel 1996 for an alternative point-of-view). For the purposes of determining the distances listed in Table 5 we assume that the halo giants discussed here are similar to those found in the dwarf spheroidals and to the "normal" carbon stars in the LMC and SMC, and hence are unlike the bright CH-type carbon stars of Hartwick & Cowley. The possibility still remains however that some or all of the halo CH stars might be similar to these brighter LMC carbon stars, in which case the distances listed for them in Table 5 should be regarded as lower limits.

We analysed the scatter in the distribution of carbon star JHK photometry using Principal Components Analysis and found that the M_K -v- $J-K$ plane produced the least scatter of any two-dimensional projection of the data (though the average of M_J, M_H, M_K was equally good). An

empirical fit of M_K with respect to $J-K$ was made and is shown plotted as the solid curve in Figure 4. The vertical scatter about the fitted curve covers a range of $\approx \pm 0.5^m$, with occasional more extreme outliers, which in the main are probably caused by variable stars. The empirical fit used has the form

$$\log_{10}(M_K + 9.0) = 1.14 - 0.65(J - K) \quad (1)$$

There are several caveats in using this to estimate the absolute K-band magnitudes, and hence distance of the Halo carbon stars. For example: even in the near infrared, dusty shells surrounding the central star will affect both the $J-K$ colour estimate and also contribute to extinction in the K-band; we have no prior way of estimating the age of the Halo carbon star population nor (easily) the intrinsic metallicity of the individual carbon stars, both age and metallicity difference can cause changes in the carbon star luminosities; many carbon stars are known to be variables and therefore without long term monitoring it is difficult to estimate the underlying "true" magnitude of this subset. However, since the compilation of carbon stars used to define the empirical relationship is likely to contain a similar spread of both age, metallicity and variable stars as the Halo population, the observed range in Figure 4 of $\approx \pm 0.5^m$ provides a realistic error range for the distance estimate of $\approx \pm 25\%$.

Equation 1 was used to estimate distances for all the FHLC star sample with extant JHK photometry and the

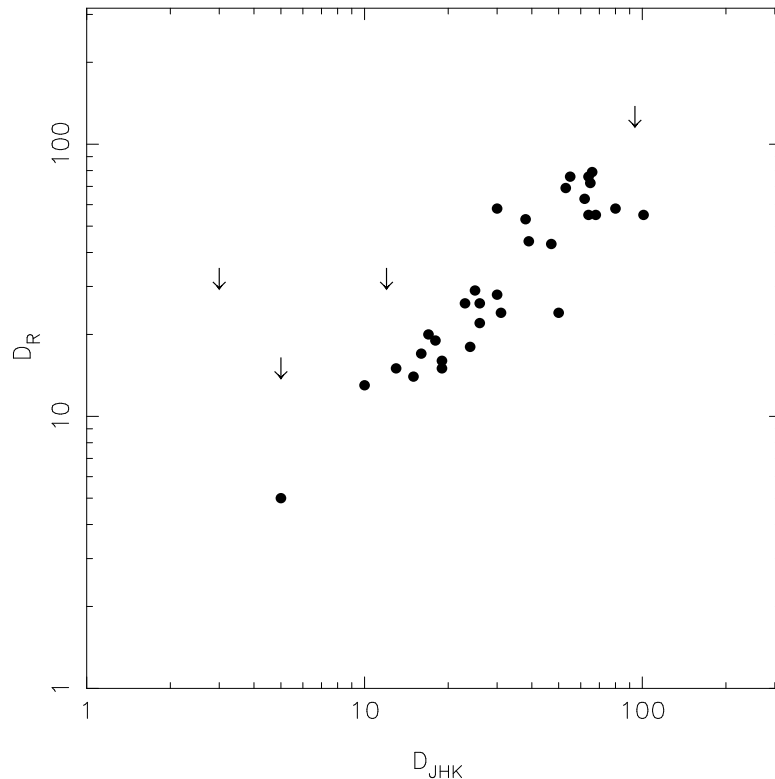


Figure 5. A comparison of distances estimated from R magnitudes against distances estimated from JHK photometry. Arrows denote those stars believed to have dusty enveloping shells, for which the distance estimated from the R magnitude is a gross over-estimation. This extinction will also affect the derived K-band distances but to a much lesser extent.

Table 4. Adopted parameters for the satellite galaxies of the Milky Way used in constructing Figure 4.

Galaxy	Distance modulus*	E(B-V)
Carina ¹	20.14	0.025 ^a
Draco ²	19.4	0.03 ^a
Fornax ³	20.59	0.03 ^b
Leo I ²	21.8	0.00 ^a
Leo II ²	21.85	0.02 ^b
LMC ⁴	18.45	0.074 ^b
Sculptor ⁵	19.47	0.02 ^a
SMC ⁴	18.80	0.03 ^a
Ursa Minor ²	19.3	0.02 ^a

Notes:

- * taken from Van den Bergh 1989.
- ^a E(B-V) taken from Aaronson & Mould 1985.
- ^b E(B-V) taken from Feast & Whitelock 1992.
- ¹ photometry from Mould *et al.* 1982.
- ² photometry from Aaronson & Mould 1985.
- ³ photometry from Aaronson & Mould 1980.
- ⁴ unpublished photometry from Irwin, Feast & Whitelock.
- photometry from Westerlund *et al.* 1995.
- ⁵ photometry from Feast & Whitelock 1992.
- photometry from Frogel *et al.* 1982 .

derived absolute K-band magnitudes, M_K and heliocentric distances for these stars are listed in Table 5.

A visual comparison between optical R-band distance estimates and JHK distance estimates is shown in Figure 5. Optically-derived distances were determined for the N-type

carbon stars (Figure 5), by assuming a luminosity of $M_R = -3.5$ (Totten & Irwin 1998). For the CH-type carbon stars however, the situation is more complicated because although the optical luminosity of cool carbon stars with optical colours of $B_J - R > 2.4$ is well approximated by a fixed luminosity in M_R , blueward of this the M_R luminosity fades rapidly with optical colour and a reliable calibration for the variation is not available. Most of the wildly discrepant points are readily explained by severe optical extinction due to surrounding dusty shells (denoted by arrows) or by variability. For the rest there is a good correlation between the optical and JHK distance estimators for the APM sample of cool carbon stars. One carbon star, 1225-0011, which we initially suspected from the optical spectrum to have a dusty envelope, probably does not, given the agreement between the optical and near infrared distance estimates. The range of Halo carbon distances derived in Table 5 extends from a small number of relatively nearby (<10 kpc) objects, typically dust enshrouded, to what appear to be normal carbon star giants ≈ 100 kpc out in the Halo of the Galaxy.

Some of the reddest carbon stars, the suspected Miras with large amplitude magnitude variations, will have uncertain derived distances. In particular, if the average magnitude is weighted by a severe fading episode which can happen for some Miras, the distances will be overestimated. More accurate distance estimates for these objects require fuller time series analysis of the light curves and will be presented elsewhere.

4 SUMMARY AND CONCLUSIONS

We have estimated proper motions for a sample of 48 carbon stars taken from Totten & Irwin (1998). Because of their intrinsically faint luminosity (Harris *et al.* 1998), dwarf carbon stars should have a relatively high and measureable proper motion compared to more distant carbon giants found in the Halo. With a $3\text{-}\sigma$ detection threshold of 21 mas/yr, our proper motion estimates show that none of the APM colour-selected carbon stars have proper motions indicative of dwarf carbon stars. A complimentary program of near infrared JHK photometry was used as further verification of carbon star type. It was found that none of the APM carbon stars lie in the region of a J-H -v- H-K plot expected to be populated by dwarf carbon stars (Westerlund *et al.* 1995) and this is taken as further proof that the sample of APM carbon stars discussed here and in Totten & Irwin (1998) are all distant carbon giants.

As a further test, proper motion measurements and extant near infrared photometry were also analysed from a previously published sample of FHLC stars and known dwarf carbon stars (Totten & Irwin 1998 Table 1.) with the purpose of verifying the existing luminosity classes of these stars and checking our proper motion measurements. It was found that one of these stars, CLS29=1037+3603 has a significant proper motion ($\mu_\alpha = 0.035 \pm 0.006$ and $\mu_\delta = -0.050 \pm 0.006$ mas/yr), indicating that it is a previously unrecognised dwarf carbon star. We have shown that CLS29 lies within the region occupied by dwarf carbon stars in a J-H, H-K two-colour diagram, confirming the implication of the proper motion measurement. CLS29 therefore appears to be an additional member of the handful of currently known dwarf carbon stars. Further examination of the space motion of CLS29, making plausible assumptions regarding the intrinsic luminosity, show that it has a Galactocentric velocity of (U,V,W) \approx (34, 210, 16) suggesting it is highly likely to be a dwarf carbon star belonging to the Galactic disk population.

Finally, by compiling a list of JHK photometry for known carbon stars in Galactic satellite dwarfs and supplementing it with SAAO JHK photometry for a large sample of cool carbon stars in the outer halos of the SMC and LMC, we have produced a calibration linking M_K and J-K for the FHLC sample. An empirical fit to this distribution was used to determine absolute K-band magnitudes for all of the FHLC stars with available JHK photometry. These absolute magnitude estimates were then used to derive approximate distances to the Halo sample of carbon stars accurate to a range of $\pm 25\%$, equivalent to a $\sigma_{dist} \approx 0.15\%$. A comparison of distances estimated from JHK observations and distances deduced from optical observations, for the mainly N-type cooler carbon stars, shows a good correlation for most of the sample. For a small subset of N-type carbon stars, the effect of extinction from a putative dusty enveloping shell is clearly seen in the differences between the JHK and the R-band derived distances, and is also apparent in the published optical spectra.

The original primary aims of the APM carbon star survey were: to find a well-defined sample of FHLC stars cov-

ering all of the high Galactic latitude sky; to prove that the majority, if not all, of these carbon stars are giants and hence members of the Halo; and to acquire accurate radial velocities together with good distance estimates for the entire sample, via JHK photometry. The survey is now complete over 3/4 of the high latitude sky; none of the newly discovered carbon stars have been found to be dwarf carbon stars; and we have accurate radial velocities and JHK photometric distances, for the majority of the sample. Interpreting the phase space structure seen in this distant Halo carbon star sample and using it as a probe of the Galactic Halo will be the subject of future papers.

5 ACKNOWLEDGMENTS

We would like to take this opportunity to thank M.W. Feast for helpful comments and for contributing to the JHK observing program, and the Director of SAAO for the use of SAAO facilities. Thanks are also due to the UKSTU for providing the plate material used in the southern part of the survey, and to members of the APM facility, past and present for maintaining such an excellent system. The CCD observations were made on the Isaac Newton Telescope which is operated on the island of La Palma by the Isaac Newton Group in the Spanish Observatorio del Roque de los Muchachos of the Instituto de Astrofísica de Canarias. This research has made use of the Simbad database, operated at CDS, Strasbourg, France.

REFERENCES

- Aaronson, M. & Mould, J., 1980, ApJ, 240, 804.
- Aaronson, M. & Mould, J., 1985, ApJ, 290, 191.
- Bessell, M. & Brett, J.M., 1988, PASP 100, 1134.
- Bothun, G., *et al.*, 1991, AJ, 101, 2220.
- Carter, B.S., 1990, MNRAS, 242, 1.
- Costa, E., & Frogel, J., 1996, AJ, 112, 2607.
- Dahn, C.C., *et al.*, 1977, ApJ, 216, 757.
- Dearborn, D.S.P., *et al.*, 1986, ApJ, 300, 314.
- Deutsch, E.W., 1994, PASP, 106, 1134.
- Feast, M.W., & Whitelock, P.A., 1992, MNRAS, 259, 6.
- Frogel, J.A. *et al.*, 1982, ApJ, 252, 133.
- Glass, I.S., 1985, IAJ, 17, 1.
- Green, P.J., *et al.*, 1991, ApJ, 380, 31.
- Green, P.J., *et al.*, 1992, ApJ, 400, 659.
- Green, P.J., *et al.*, 1994, ApJ, 434, 319.
- Green, P.J., 1996, I.A.U. Symp. 177: The Carbon Star Phenomenon.
- Hartwick, F.D.A. & Cowley, A.P., 1988, ApJ, 334, 135.
- Harris, H.C., *et al.*, 1998, ApJ, 502, 437.
- Heber, U., *et al.*, 1993, A & A, 267, 31.
- Irwin, M.J., *et al.*, 1990, AJ, 99, 191.
- Irwin, M.J., & McMahon, R., 1992 Gemin., 36, 1.
- Irwin, M.J., *et al.*, 1994, Spectrum No.2, p14.
- Irwin, M.J., & Totten, E.J., 1999 in prep.
- Irwin, M.J., 1999, private communication.
- Kibblewhite E.J., *et al.*, 1984, in *Proc. Astronomical Microden-*
sitometry Conference. NASA-2317 p277.

- Moody, J.W., *et al.*, 1997, AJ, 113, 1022.
Mould, J.R., *et al.*, 1982, ApJ, 254, 500.
Phillips, M.M., Terlevich, R., 1983, PASP, 95, 43.
Sanduleak, N., & Pesch, P., 1988, ApJSupp, 66, 387.
Stephenson, C.B., 1989, Publ. Wanere & Swasey Obs., VOL 3,
no.2.
Suntzeff, N.B., *et al.*, 1993, PASP, 105, 350.
Totten, E.J., & Irwin, M.J., 1998, MNRAS, 294, 1.
Van den Bergh, S., 1989, A & AR, 1, 111.
Westerlund, B.E., *et al.*, 1995, A & A, 303, 107.